https://doi.org/10.26682/sjuod.2023.26.1.14
Journal of University of Duhok., Vol. 26, No.1 (Pure and Engineering Sciences),Pp 139-149, 2023

PREPARATION OF SILVER NANO-PARTICLES IN BENZENE SOLVENT BY LASER ABLATION METHOD

MUHAJ TALIB ABAULLAH
College of Science, University of Zakho, Kurdistan Region-Iraq

(Received: October 16, 2022; Accepted for Publication: April 16, 2023)

ABSTRACT

Nd-yag laser with wavelength (λ) =1064nm and energy 1100 mJ was used to prepare Ag nano particles in aromatic solvent benzene for the first time in this work according to our knowledge. UV–Vis spectroscopy, X-ray diffraction (XRD), (EDX), TEM, FTIR, Photoluminescence measurement, and Raman shift were used to examine the optic, structural, as well as morphological features of Ag Nano particles. According to XRD patterns, the synthesized Ag NPs exhibit a nanocrystalline and cubic (FCC) structure. The direct optical energy gap of Ag NPs discovered to be within the range of (2.8) eV. The Photoluminescence emission spectra and excitation spectra of Ag the emission peak fixed around 380 and 430 nm respectively. When the findings from the experiment are compared to those from the reference sample, it becomes clear that benzene has substantially higher nanoparticle production efficiency and smaller particle sizes.

KEYWORDS: Silver nanoparticles, Laser ablation. Benzene solvent, plasmon peak, pulsed laser ablation in liquids.

1-INTRODUCTION

The preparation of metallic nanoparticles employs a unique, practical, and an important process called laser ablating of bulk materials immersed in a solutions. Because this method is characterized by versatility and simplicity of use, it produces clean as well as unpolluted metal nanoparticles with no need for various chemicals in solution. [1-8]. Ablating efficiency and features of created nano-silver particles are strongly influenced by a number of elements, such as the laser's wavelength that impinges the target, the effective liquid medium, the ablation time duration, the laser power in addition to the presence or the absence of surfactants [9,10]. The productive of laser ablation in liquid (LAL) can be improved via used of a liquid flow, by choosing a low liquid level, and by performing LAL in water. In specific cases, water undesirably alters the properties of the NPs, for instance, by oxidation. Low-viscous organic solvents represent the best alternatives in such a case [44]. There are other studies that dealt with the effect of organic solvents on the optical properties of ultra-small particles prepared by laser ablation in solutions [45]. Nanomaterials have recently piqued the interest of scientists due to their unique and crucial features as compared to bulk materials. The characteristics of the material dramatically change when the size of the component particle reaches the nanoscale realm. Nanoparticles' characteristics can mostly be determined by their size and form. They include noble metallic nanoparticles like Ag, Au, Pt, as well as Pd, which have uses in biological, chemic, and physical processes. [11,12]. Ags an example of transition metal, silver is a soft, white, glossy element that is within a set with copper plus gold. Ags have good electrical, optical, and thermal properties [13–15]. Silver nanoparticles (AgNPs) have being employed more often in a wide range of industries, such as medicine, health care, food manufacturing, and consumer products, as a result of their unique physic as well as chemic properties. AgNPs have been employed as antibacterial factors, in orthopedics, drug administration, diagnostics, also as anticancer factors, eventually enhancing the tumor-killing actions of anticancer medications. [16]. Improving AgNPs production efficacy and reducing particle sizes. As opposed to that, the synthesized AgNPs in benzene solutions have more stability for a long time. By interacting with hydroxyl groups, ion-dipoles in benzene prevent the AgNPs from forming clumps [17], which is how it prevents agglomerate (–OH).

The purpose of this work is to investigate the structural, morphological, and optical properties of Ag NPs prepared using the PLAL technique and using the benzene as a medium.

MATERIALS PLUS CHEMIC REAGENTS

An order for 99.99% of pure Ag plates was made via (www.np-laser.com) to Zhongke (Hefei) Napu New Materials Co. Ltd. Additionally, the ormatic solvent of benzene was obtained from the University of Technology's Chemistry Branch of the Department of Applied Sciences

Experimental part

Pulsed YAG laser ablating was used to create Ag nanoparticles from pure silver (99.999% pureness) that was put in an aromatic solvent-filled beaker (benzene) [17]. The Nd-YAG laser employed there has a wavelength, energy, and pulse count of 1064 nm, 1200 mJ, and 2000–2500 beats per second, respectively. The beam diameter is 2.3 mm. At room temperature, the ablation process took around 25 minutes. The colloidal solution of silver nanoparticles was obtained; this was visually revealed by changing the solution's colour from transparent white to golden yellow. The flexible synthetic method known as the Laser Ablating in Liquid (LAL) allows for the quick synthesis of nanoparticles from simple starting materials. LAL works by focusing an intensive laser beam into a liquid or onto a solid-liquid interface. Traditional wet-chemical approaches for preparing colloidal nanoparticles and nanocomposite materials have a number of disadvantages as compared to LAL processes. In comparison to hours or days generally required with older procedures, for just a few minutes of laser process and minimal post-synthetic work-up, LAL produces significant amounts of nanoparticle products. Figure 1 also depicts the experimentation setup for laser ablating of a silver target submerged within benzene.

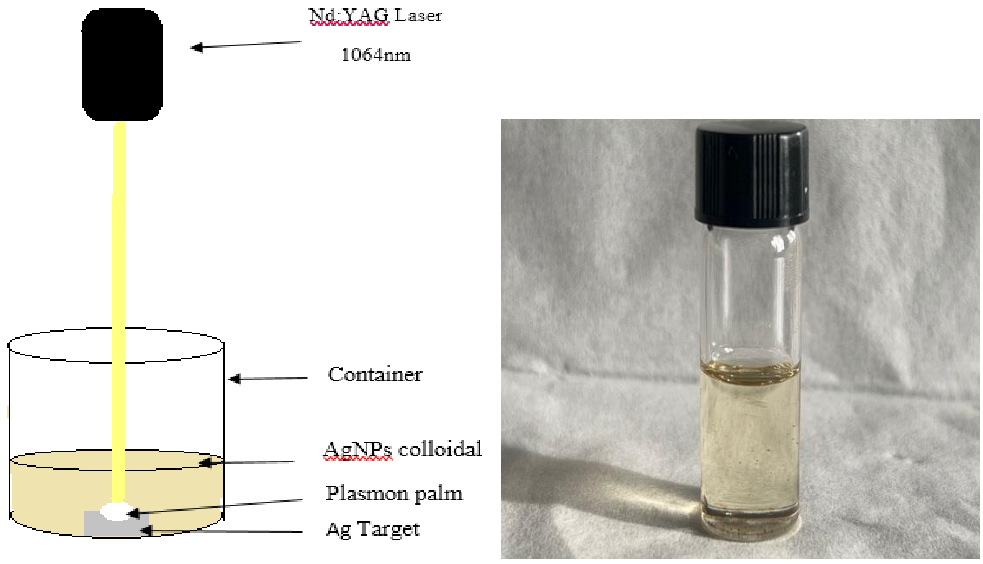

Fig. (1): Schematic diagram of the laser ablating technique on the left and Colloidal of` silver nanoparticles on the right

Characterization

The UV/VIS spectra were collected using a Perkin Elmer Lambda 365 UV/VIS spectrometer. The FluroMate FS-2 Spectrometer's PL Lamp System was used to capture the photoluminescence (PL). The X-ray diffracting (XRD) spectrometer, model number XRD-6000, SHIMADZU, Japanese, operates at 220 V/50 Hz., While the Bruker Company/ GermanyXFlash 6l10/Model was used to get EDX (Energy Dispersive X-Ray Spectroscopy). By utilizing Model Spectrum TWO, Fourier Transform Infra-red (FT-IR) analysis was performed (Perkin Elmer). and by Utilizing a PHILIPS brand CM10, Transmitting Electronic Microscopy (TEM) was conducted, and Raman was acquired using a system with a preconfigured 532 nm Raman spectrometer system.

RESULTS AND DISCUSSION

A popular analytical method for determining particle sizes and levels of crystallinity in molecules as well as crystal structures is X-ray diffraction (XRD). Ag nanoparticles with cubic (fcc) crystal structure and the three main peaks located at 38.18°, 44.25°, and 64.55°, respectively, correlating to the (111), (200), and (220) planes, are produced by laser ablation in benzene and deposited on glass substrate by drop casting. The X-ray diffraction pattern of these Ag nanoparticles is shown in Figure 2 and is confirmed by comparison with JCPDS Card No. 04 [18-21].

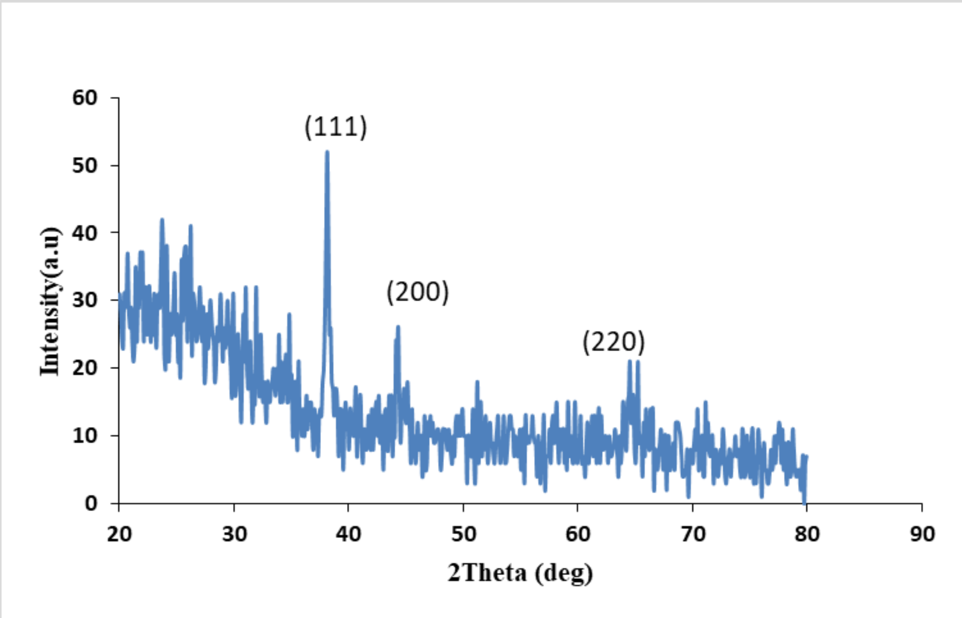

Fig. (2): XRD analysis of silver nanoparticles

This result agrees with the result obtained from their reference [22].

Peaks that represent the planes at 111, 200, and 220, correspondingly, have values of 38.06, 44.23, and 67.43. Those planes demonstrated that the extract-produced AgNPs were crystalline in character.

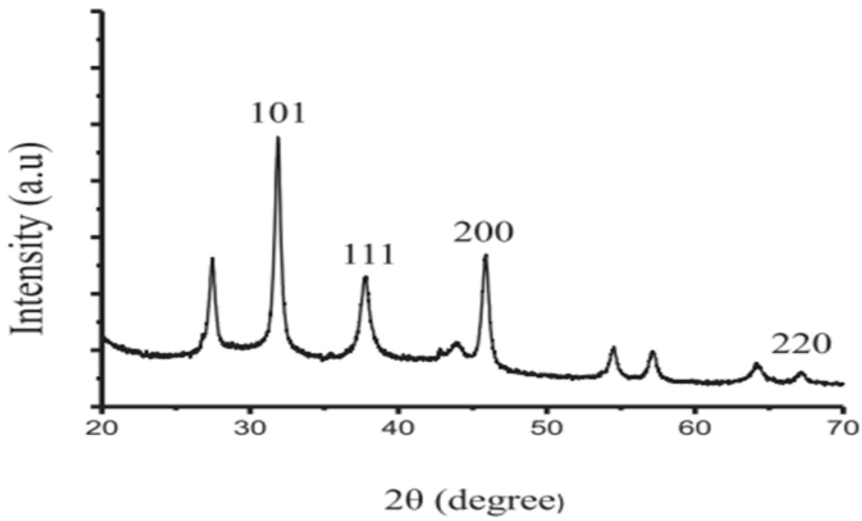

Fig. (3): XRD graph represents the crystalline nature of silver nanoparticles. [15]

And the XRD pattern for the produced AgNPs in other papers [23]. The face-centered cube (fcc) structure of metal silver having a space group of Fm-3m was indexed to the detected diffracting peaks at 37.98_, 44.17_, 64.38 and 77.3 in the 2h scope which correspond to (111), (200), (220), and (311) reflecting planes (JCPDS 04-0783) [23].

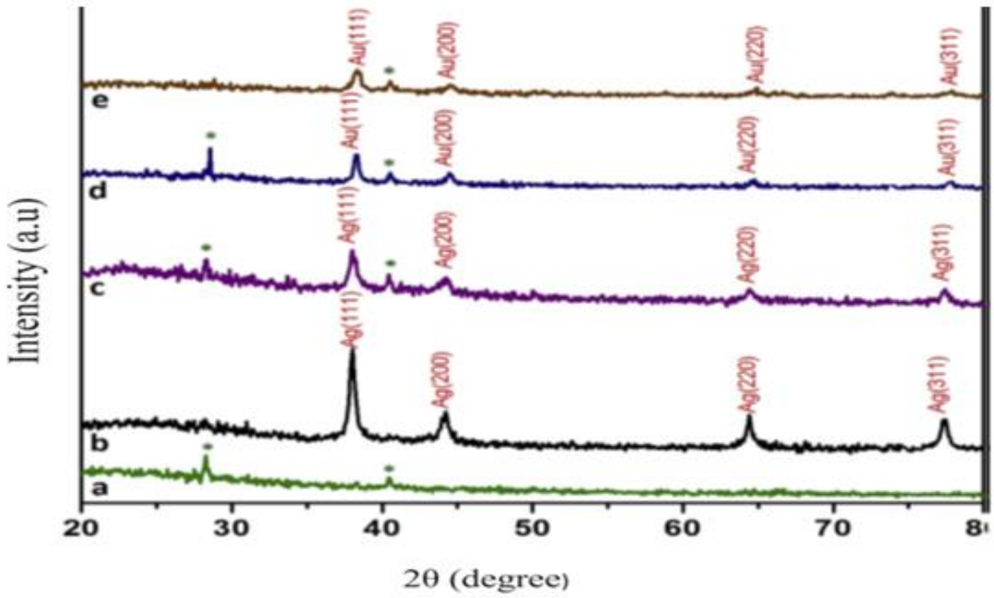

Fig. (4) : shows the EDX spectrum. The elements found in the normal count were Si=28.36, Ag=28.02, Na=5.16, Ca=4.98, Mg=1.27, Cl=0.76, and S=0.61.

The apparent existence of Ag peaks at 3 KeV, which are the characteristic absorption peak of the silver nanocrystals, is demonstrated by the EDX spectrum of Ag nanoparticles. Because of the silicon wafer existence, which served as an Ag support, the Si peak at 1.75 KeV could similarly be observed. The carbon signals is due to the surfactant. Showed strong noise signals including Ca, Na S, Al and Mg; this may be due to the presence of impurities in benzene [24-26]

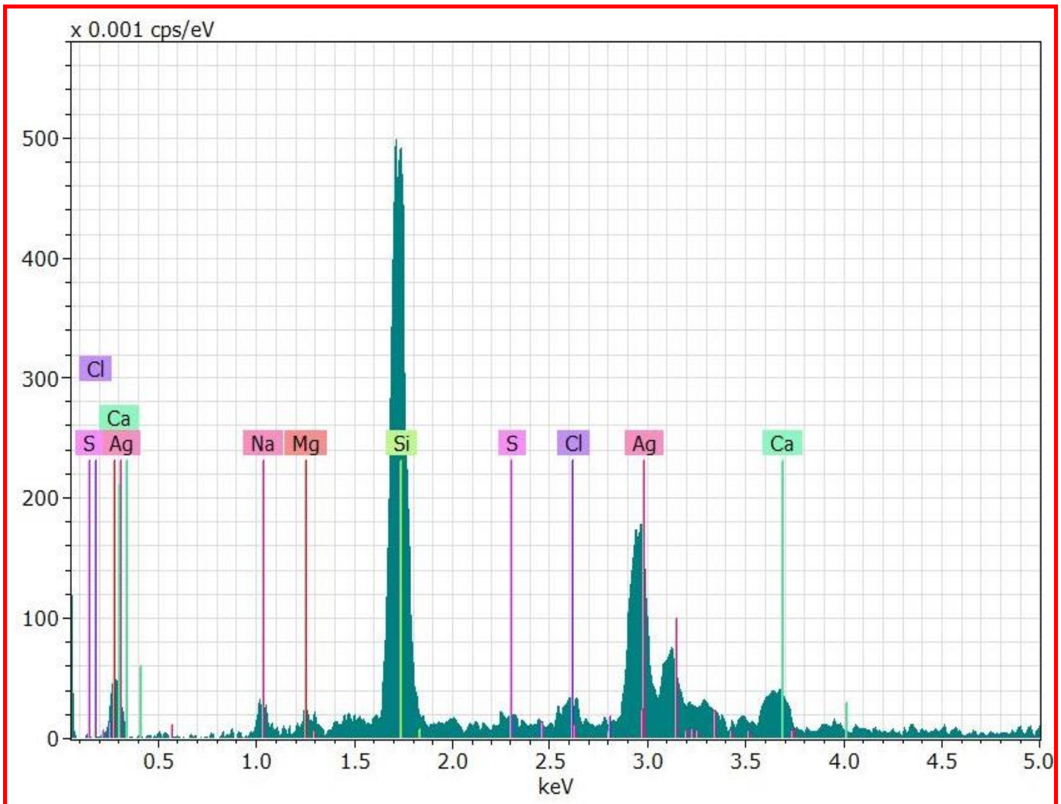

Fig. (5): EDX of silver nanoparticls

UV–visible spectroscopy studies of Ag NPS

UV-Vis analysis was performed. to carry out the initial characterization of Ag nanoparticls and their oxides are two types of nanoparticles. Figure 4 displays a UV–Vis spectra of the colloidal solvent of silver nanoparticles prepared by laser ablation in benzene at range (200-1100) nm. At the laser wavelength of 1604 nm, an optic absorbing band having a maximum at 310 nm was discovered. This is a characteristic of the absorbing of metal silver nanoparticles caused by the Surface Plasmon resonances (SPR), demonstrating the existence of Ag nanoparticles inside the solvent. [27-30]. The colloidal solution contains particles of various sizes coexist, as shown by a wide absorbance band.

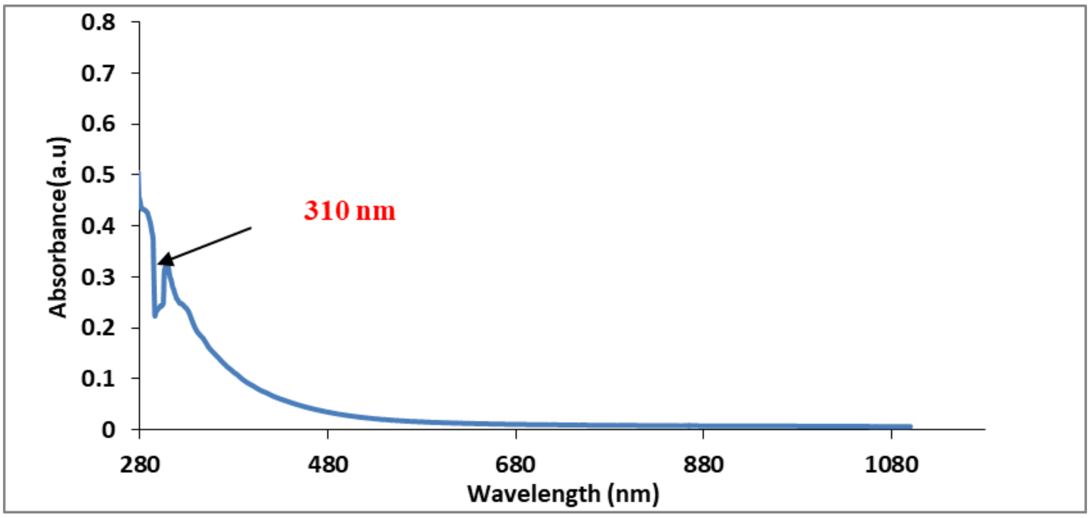

Fig. (6): The UV-visible of silver nanoparticles

Intense Plasmon band absorbance at 310 nm and modest inter-band absorbance in the 200–250 nm range are present in the spectra, respectively. Within our circumstances, an analysis of the absorption of inter-band transition at 250 nm shows that the production efficiency of colloids rises along with an increasing within the laser wavelength. This was explained according to the prior reports. [24]

The tiny, spheric nanoparticles' production and uniform dispersion are shown by the blue-shifted, narrow SPR band [31]. The obvious peaks at 310 nm in the absorbance spectra showed a tendency to blue shift; such peak could be attributed to the impact of quantum size [17]. These absorbance maxima are associated with NPs that are spherical (or almost spherical) and have an average diameter that is typically around 2 and 100 nm [32]. TEM pictures and the accompanying statistical and morphological analysis were used to confirm such findings. The energy gap was estimated using the equation of energy, as follows:

$E = h \times c/\lambda$

$h = 6.626 \times 10^{-34}$, $c = 3 \times 10^{8}$ m/s

In the SI system, the Planck variable h is expressed within Joule-seconds, and Electronvolt (eV) within the M.K.S system, .1 eV = 1.6×10^{-19} Joule

$E=(1240/\lambda)$ ev for λ in nm

The curve was drawn between the value of the absorbance multiplied by the value of the wavelength in micrometers on the y-axis and the value of the energy gap, which was calculated according to the above eq. The energy gap was calculated as a result of the intersection of the drawn lines aligned with the obtained curve as illustrated in Figure 5 [33-34], and its equal to 2.8 eV, this result agrees with the Ehab Mohammed Ali research [35]. The optical absorption of metal nanoparticles (MNPs) may be accounted for quantum mechanically, simulating light interactions on metal surfaces through photoelectric absorbance plus Compton scatter. This is because intra-band conduction electrons are excited via photons. [30-33]. While some conduction electrons in MNPs are held by particular atoms, others are loose and can move across atoms to create metallic connections that hold the metallic nanoparticles together. When photon energy of UV lighting with the maximum absorbing wavelengths (max) is applied, the conduction electrons undergo intra-band quantum excitation above the Fermi energy level, which is where the conduction band of metallic nanoparticles can be determined. The possibility of an attraction amid the metallic ions and the particle's conduction electron is reduced with smaller particle sizes. As a result, the smaller particle's conduction band energy rises. Larger particle sizes, on the other hand, include a greater number of atoms, which increases the attracting possibility amid conduction electrons with metallic ions, lowering the energies of metallic nanoparticles' conduction bands [36].

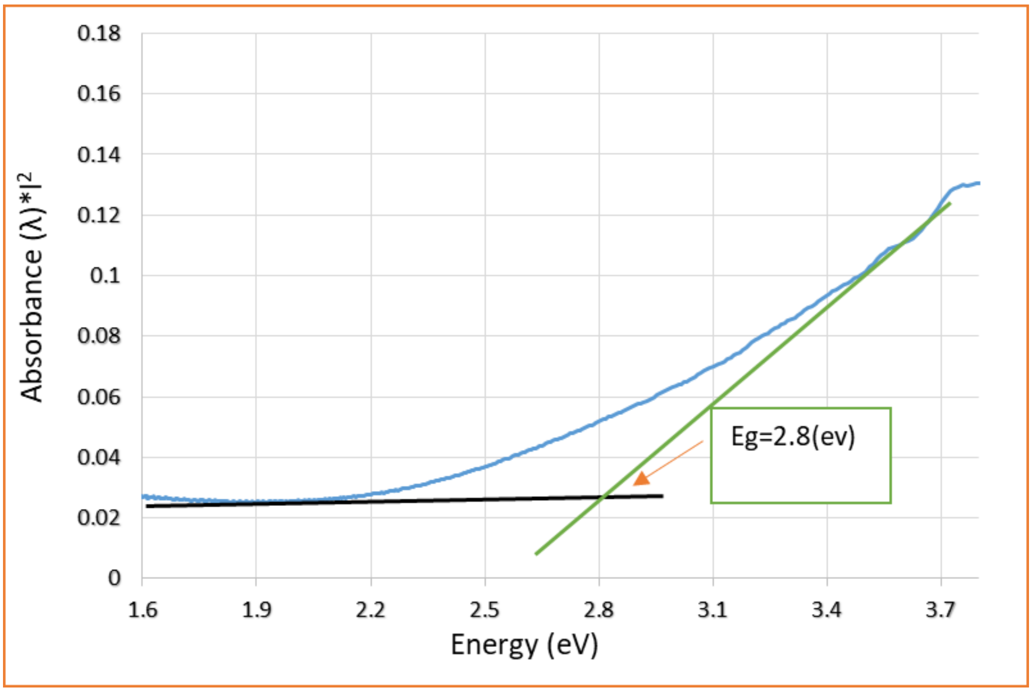

Fig. (7): Tauc plot of Ag Quantum dots

The TEM analyzing verified the existence of nanoscale particles. The average diameter of the particles, which ranged from 3 to 24 nm, was less than 10 nm, and they had a spherical form. Ag nanoparticles prepared by leaser ablating within benzene with energy of (1100 mJ) are shown in the TEM image and the number of pulses is 2000-2500 beats/second. The development of aspheric, monodispersed nanoparticles was depicted in Figure 6 by the TEM imaging. Metal nanocrystals with an Fcc structure have a propensity to form twin particles and have least energy facets around their surface (111) [27]. The distributing of particle sizes in Fig. 8b is depicted as having an average size of 9 nm and a range of 3 to 24 nm. The particles are either aspheric or elliptic in form.

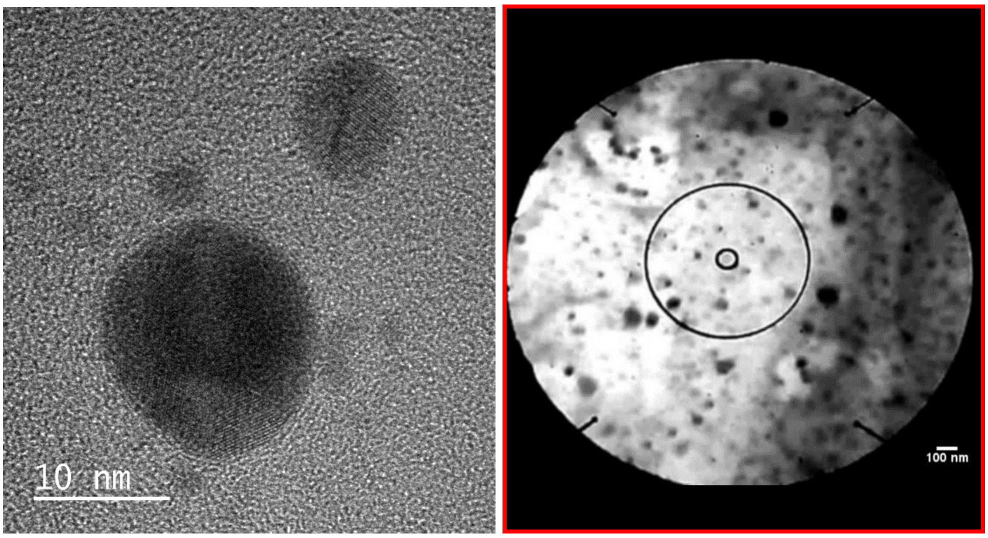

Fig. (8a): TEM analysis of silver nanoparticles

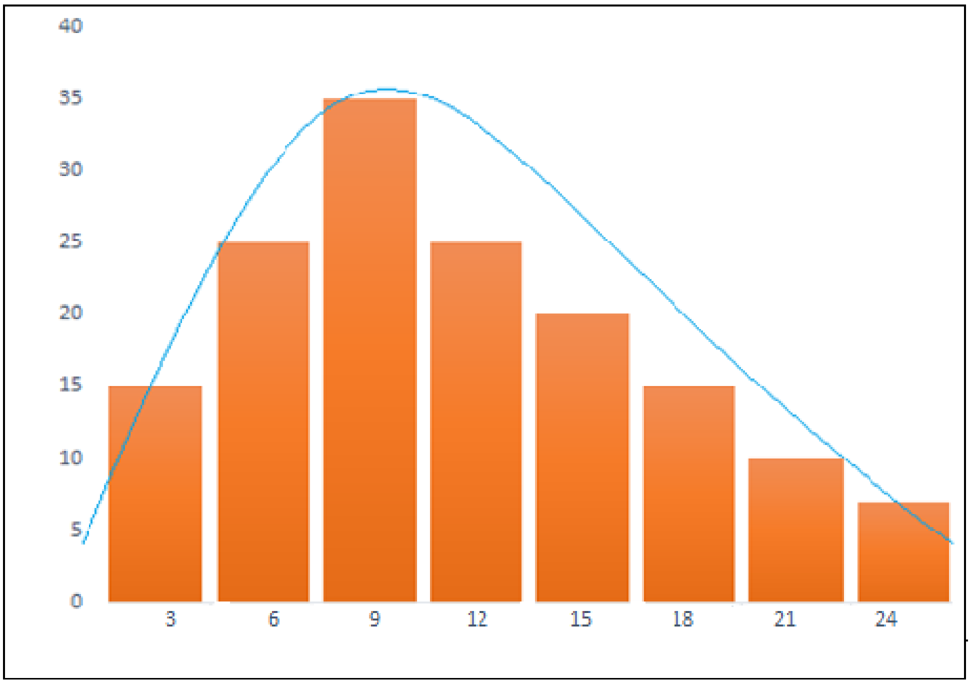

Fig. (8b): the particle size distribution of Ag

The FTIR spectra of silver nanoparticles produced via leaser ablation in benzene are shown in Figure 9. Different absorbance peaks were identified by Ag nanoparticle FTIR data, which helped assign the various functioning groups of phytochemicals. The O=H stretching of phenolic compounds, N-H stretching of prime as well as secondary amines plus amides, C=H stretching of methyl groups, C=C stretching of alkynes, H-C=O: stretching of aldehydes, and C=O stretching of carbonyl groups of flavonoids and tannins, correspondingly, were assigned to the absorbance peaks at 3739, 3321, 2916, 2371, 1958, and 1656 cm 1. [22] Also The peak at 1357 cm^{-1} is representing the C=N stretch of nitriles. The peak 1104 cm^{-1} correlates to C–O stretch. The peaks observed at 845, 751, 665 and 604 cm^{-1} correlate to C–H stretch of alkenes. Whereas the peak for Ag-NPs was found around 594 cm^{-1}**[39-41]**

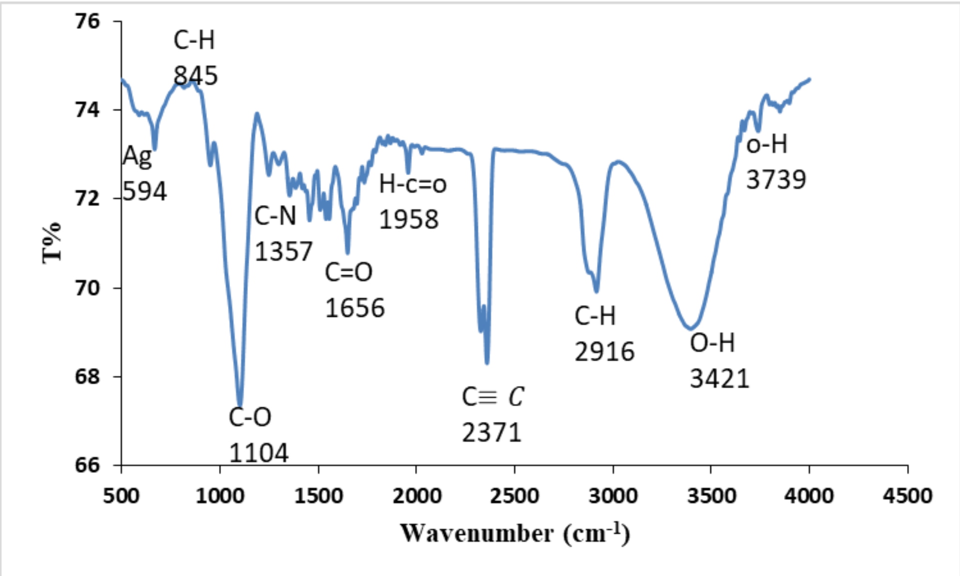

Fig. (9): FTIR spectrums of Ag NPs by laser ablation method.

Figure 10 shows the Photoluminescence emission and excitation peak of Ag NPs which created by laser ablating in benzene. The red-band area of the emission spectrum has a single strong peak that represents the basic absorbance of silver nanoparticles. The peak's center at 430 nm is attributable to electrons from gold nanoparticles that are quantum-confined. It was detected at around 430 nm, where a shift in the emission peak at a shorter wavelength was observed, this indicates a blue shift [22], and the excitation spectrum is detected with a strong and intensive peak concentrated at 370 nm, where the energy gap is measured, it is found to be equal to 2.88 eV at 430 nm, this is the same value as that obtained from UV-Vis measurement [42].

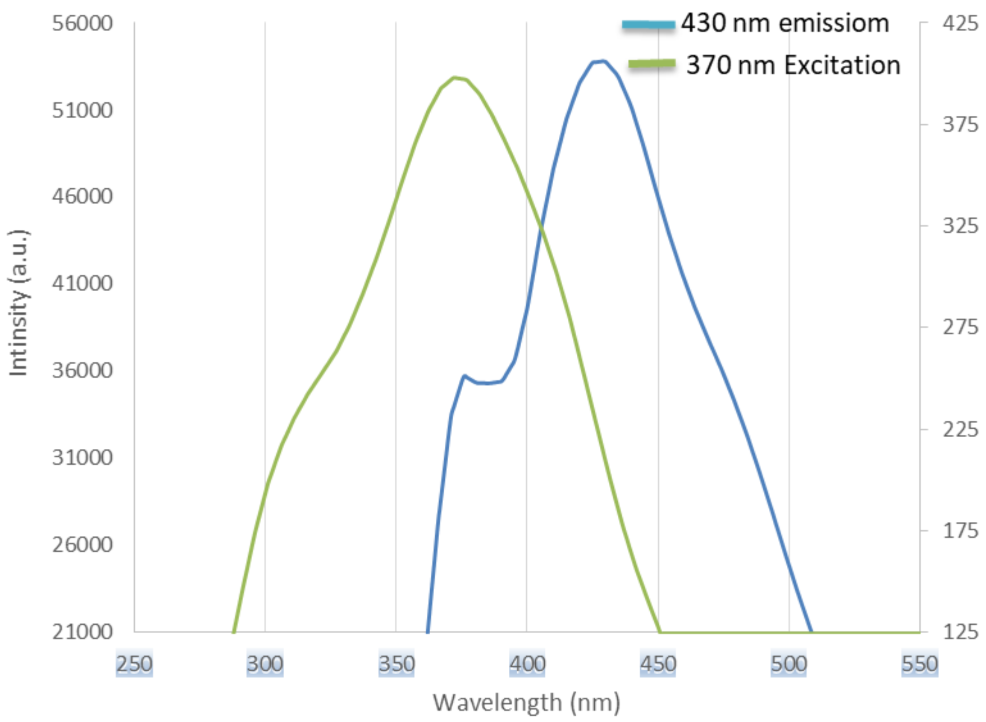

Fig. (10): Photoluminescence emission and excitation peak of Ag NPs

Raman spectra of silver nanoparticles are shown in Figure 11. They consist of vibrational modes at 890-1407 cm^{-1} for Ag NPs [43] mode. The Raman signals at 1153 cm^{-1} arise from modes of in-plane C-C stretching vibrations and 3315 cm-1of O-H stretching vibrations. The other band at 1882 cm^{-1} is obtained due to C=O stretching vibration of carboxylic group .

For the purpose of determining the chemical structure of the silver nanoparticles, Raman spectra were gathered. Raman scatter has established itself as a key method for learning about the local structures of various nanoparticles. Impurity detection cannot be totally disregarded because of the great sensitiveness of detecting for Raman active species, particularly because displayed characteristics in the CH stretch area are challenging to interpret. According to the results of the Raman spectra of the Ag nanoparticles, an Ag-O mode could be attributed to a vibrating band at 250 centimeters, and an Ag mode could be attributed to a vibrating band at 1050 centimeters. The wide band at 820 cm-1 can be attributed to N, N-dimetylformamide-derived O=C-N vibrating.

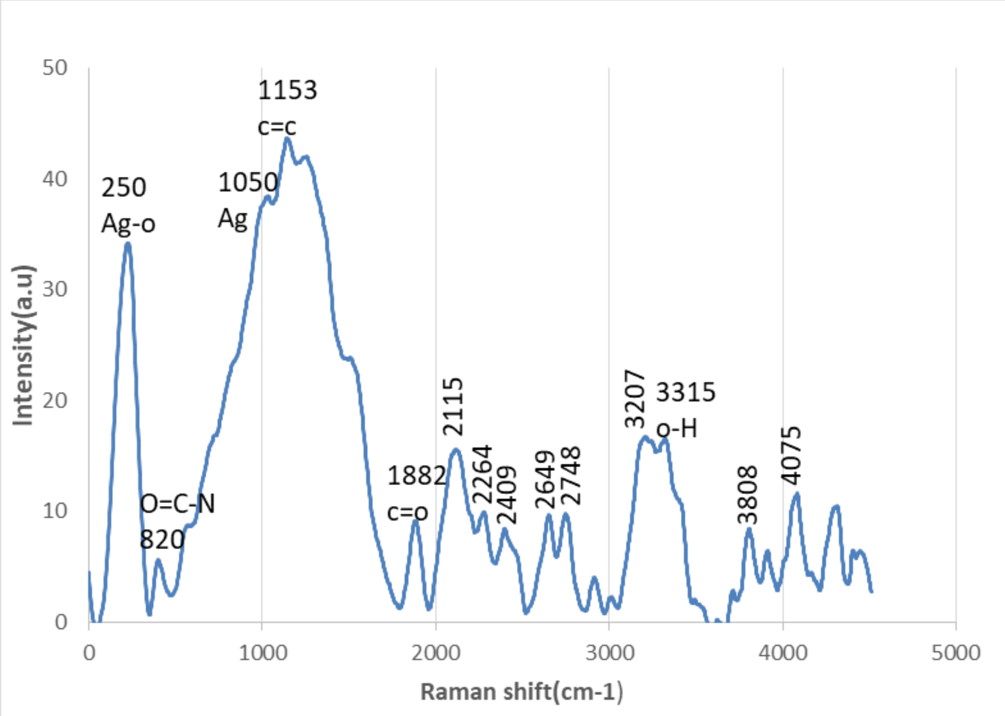

Fig. (11): Raman spectra of silver.

CONCLUSION

To sum up, The Ag NPs in benzene solution have effectively been manufactured utilizing the laser ablation approach. The formation effectiveness of NPs is enhanced along with decreasing particle sizes. As a consequence of the current work, it is the first time that the synthesis of the silver nanoparticles as well as the impact of benzene concentrations on their characteristics have been described. also, the present work showed that it is possible to obtain AgNPs by laser ablation in benzene. The achieved results show that cubic Ag-phase with spherical shape particles forms at the nanoscale with an energy gap of 2.8 eV. These results indicate the possibility of using Ag NPs in many applications (for future work) such as drug administration, diagnostics, also as anticancer factors, eventually enhancing the tumor-killing actions of anticancer medications.

REFERENCES

Hisham Imam1, Khaled A.Elsayed2, Lotfi Z. Ismail2, Mostafa Afify2 and M. Atta Khedr1"Fabrication of Silver Nanoparticles by Laser Ablation in Liquid Solution" Life Science Journal (2013). http://www.lifesciencesite.com.

Pastoriza-Santos, L.M. Liz-Marzan, [Synthesis of silver nanoprisms in DMF] Nano Lett. 2 (2002). https://doi.org/10.1021/nl025638i

Ahmed N. Abd1 • Raid A. Ismail2 • Nadir F. Habubi "Characterization of CdS nanoparticles prepared by laser ablation in methanol " J Mater Sci: Mater Electron (2015). https://doi.org/10.1007/s10854-015-3660-5

M. Tsuji, M. Hashimoto, Y. Nishizawa, M. Kubokawa, T. Tsuji, [Microwave-Assisted Synthesis of Metallic Nanostructures in Solution] Chem. Eur. J. 11 (2005). https://doi.org/10.1002/chem.200400417.

Xi-Feng Zhang 1, Zhi-Guo Liu 1, Wei Shen 2 and Sangiliyandi Gurunathan "Silver Nanoparticles: Synthesis, Characterization, Properties, Applications, and Therapeutic Approaches" Int. J. Mol. Sci.(**2016)**. http://doi: 10.3390/ijms17091534.

B. Wiley, Y. Sun, B. Mayers, Y. Xia, [Shape-Controlled Synthesis of Metal Nanostructures: The Case of Silver] Chem. Eur. J. 11 (2004). https://doi.org/10.1002/chem.200400927

B.J. Wiley, S.H. Im, Z.Y. Li, J. McLellan, A. Siekkinen, Y. Xia, Maneuvering the surface plasmon resonance of silver nanostructures through shape-controlled synthesis, J. Phys. Chem. B 110 (2006). https://doi.org/10.1021/jp0608628

S. Iravani, H. Korbekandi, S.V. Mirmohammadi, B. Zolfaghari, Synthesis of silver nanoparticles: chemical, physical and biological methods, Research in Pharmaceutical Sciences 9 (2014). https://www.ncbi.nlm.nih.gov/pmc/articles/PMC4326978

N. Tarasenko, A. Butsen, E. Nevar, N. Savastenko, Synthesis of nanosized particles during laser ablation of gold in water, Appl. Surf. Sci. 252

(2006). https://doi.org/10.1016/j.apsusc.2005.07.150

M. Kawasaki, N. Nishimura, Laser fragmentation of thin Au and Ag flakes in acetone for highly productive pathway to stable metal nanoparticles, Appl. Surf. Sci. 253 (2006). https://ui.adsabs.harvard.edu/abs/2006ApSS..253.2208K

S. Prabhu, E.K Poulose, Silver nanoparticles: mechanism of antimicrobial action, synthesis, medical applications and toxicity effects, Int. Nano Lett. 2 (2012). https://link.springer.com/article/10.1186/2228-5326-2-32

S. Ghosh, S. Patil, M. Ahire, R. Kitture, S. Kale, K. Pardesi, S.S. Cameotra, J. Bellare, D.D Dhavale, A. Jabgunde, B.A. Chopade, Synthesis of silver nanoparticles using Dioscorea bulbifera tuber extract and evaluation of its synergistic potential in combination with antimicrobial agents, Int. J. Nanomedicine 7 (2012). DOI: 10.2147/IJN.S24793

Gurunathan, S.; Park, J.H.; Han, J.W.; Kim, J.H. Comparative assessment of the apoptotic potential of silver nanoparticles synthesized by Bacillus tequilensis and Calocybe indica in MDA-MB-231 human breast cancer cells: Targeting p53 for anticancer therapy. Int. J. Nanomed. (**2015**). doi: 10.2147/IJN.S83953

Li,W.R.; Xie, X.B.; Shi, Q.S.; Zeng, H.Y.; Ou-Yang, Y.S.; Chen, Y.B. Antibacterial activity and mechanism of silver nanoparticles on Escherichia coli. Appl. Microbiol. Biotechnol. (**2010**). doi: 10.1007/s00253-009-2159-5

Mukherjee, P.; Ahmad, A.; Mandal, D.; Senapati, S.; Sainkar, S.R.; Khan, M.I.; Renu, P.; Ajaykumar, P.V.; Alam, M.; Kumar, R.; et al. Fungus-mediated synthesis of silver nanoparticles and their immobilization in the mycelial matrix: A novel biological approach to nanoparticle synthesis. Nano Lett. (**2001**). https://doi.org/10.1021/nl0155274

Chernousova, S.; Epple, M. Silver as antibacterial agent: Ion, nanoparticle, and metal. Angew. Chem. Int. Ed.(**2013). https://doi.org/10.1002/anie.201205923**

Abdulrahman K. Ali1,2 · Sule Erten‑Ela1 · Raid A. Ismail2 · Cagdas Yavuz1

"Preparation of blue luminescence gold quantum dots using laser ablation in aromatic solvents"Applied Nanoscience https://doi.org/10.1007/s13204-021-02171-1

Das, R.; Nath, S.S.; Chakdar, D.; Gope, G.; Bhattacharjee, R. Preparation of silver nanoparticles and their characterization. J. Nanotechnol. (**2009**). DOI : 10.2240/azojono0129

Waseda, Y.; Matsubara, E.; Shinoda, K. X-ray Diffraction Crystallography: Introduction, Examples and Solved Problems; Springer Verlag: Berlin, Germany, (2011). https://link.springer.com/book/10.1007/978-3-642-16635-8

Ananias, D.; Paz, F.A.; Carlos, L.D.; Rocha, J. Chiral microporous rare-earth silico-germanates: Synthesis, structure and photoluminescence properties. Microporous Mesoporous Mater. (**2013**). 10.1016/j.micromeso.2012.04.032

Xu, Z., Hou, Y. and Sun, S. ‘‘Magnetic core/shell Fe3O4/Au and Fe3O4/Au/Ag

nanoparticles with tunable plasmodic properties’’, J. Am. Chem. Soc., 129,

pp. 8698–8699 (2007). https://doi.org/10.1021/ja073057v

Anand Kumar Keshari a, Ragini Srivastava a, *, Payal Singh a, Virendra Bahadur Yadav b, Gopal Nath "Antioxidant and antibacterial activity of silver nanoparticles synthesized by Cestrum nocturnum"Journal of Ayurveda and Integrative Medicine xxx (2018). DOI:10.1016/j.jaim.2017.11.003

M.R. Bindhu, M. Umadevi "Silver and gold nanoparticles for sensor and antibacterial applications" Spectrochimica Acta Part A: Molecular and Biomolecular Spectroscopy 128 (2014) 37–45. DOI: 10.1016/j.saa.2014.02.119

Saware K, Sawle B, Salimath B, Jayanthi K, Venkataraman A. Biosynthesis and characterization of silver nanoparticles using Ficus Benghalensis leaf extract. Int J Res Eng Technol (2014).

https://ijret.org/volumes/2014v03/i05/IJRET20140305158.pdf

Soumya Menon, Happy Agarwal, S. Rajesh Kumar, S. Venkat KumaR "Green Synthesis Of Silver Nanoparticles Using Medicinal Plant Acalypha Indica Leaf Extracts And Its Application As An Antioxidant And Antimicrobial Agent Against Foodborne Pathogens ", International Journal of Applied Pharmaceutics (2017).

https://doi.org/10.22159/ijap.2017v9i5.19464

Maryam Abdollahnia1 , Ali MakhdoumiID1 *, Mansour Mashreghi1,2, Hossein Eshghi "Exploring the potentials of halophilic prokaryotes from a solar saltern for synthesizing nanoparticles: The case of silver and selenium ", PloS one (2020). DOI: 10.1371/journal.pone.0229886

D. Kim, S. Jeong, J. Moon, Synthesis of silver nanoparticles using polyol process and the influence of precursor injection, Nanotechnology 17 (2006). doi: 10.1088/0957-4484/17/16/004

K.J. Lee, B.H. Jun, J. Choi, Y.I. Lee, J. Joung, Y.S. Oh, Environmentally friendly synthesis of organic-soluble silver nanoparticles for printed electronics, Nanotechnology 18 (2007). **DOI** 10.1088/0957-4484/18/33/335601

G.K. Vertelov, Y.A. Krutyakov, O.V. Efremenkova, A.Y. Olenin, G.V. Lisichkin, A versatile synthesis of highly bactericidal Myramistin stabilized silver nanoparticles, Nanotechnology 19 (2008). DOI: 10.1088/0957-4484/19/35/355707

Y.A. Krutyakov, A.A. Kudrinskiy, A.Y. Olenin, G.V. Lisichkin, Synthesis and

properties of silver nanoparticles: advances and prospects, Russ. Chem. Rev. 77

(2008). http://dx.doi.org/10.1070/RC2008v077n03ABEH003751

K.R. Brown, D.G. Walter, M. Natan, , **Seeding of Colloidal Au Nanoparticle Solutions. 2. Improved Control of Particle Size and Shape** Chem. Mater. 12 (2000) 306–313. **https://doi.org/10.1021/cm980065p**

Burda, C.; Chen, X.; Narayanan, R.; El-Sayed, M.A. Chemistry and properties of nanocrystals of different shapes. *Chem. Rev.* **2005**, *105*, 1025–1102. https://doi.org/10.1021/cr030063a

Saion, E.; Gharibshahi, E. On the theory of metal nanoparticles based on quantum mechanical calculation. J. Fundam. Sci. (2011). DOI:10.11113/mjfas.v7n1.202

Soltani, N.; Saion, E.; Erfani, M.; Rezaee, K.; Bahmanrokh, G.; Drummen, G.P.; Bahrami, A.; Hussein, M.Z. Influence of the polyvinyl pyrrolidone concentration on particle size and dispersion of ZnS nanoparticles synthesized by microwave irradiation. Int. J. Mol. Sci. (2012). doi: 10.3390/ijms131012412

Ehab Mohammed Ali, Khetam H.Rasool, Wedian K. Abad, Ahmed N. Abd "Green Synthesis, Characterization and Antimicrobial activity of CuO nanoparticles (NPs) Derived from Hibiscus sabdariffa a plant and CuCl", J.Physics and Applied Sciences ICPAS (2021). **DOI** 10.1088/1742-6596/1963/1/012092

Leila Gharibshahi , Elias Saion , Elham Gharibshahi, Abdul Halim Shaari and Khamirul Amin Matori "Structural and Optical Properties of Ag Nanoparticles Synthesized by Thermal Treatment Method", Materials (2017). doi: 10.3390/ma10040402

Barone, P.; Stranges, F.; Barberio, M.; Renzelli, D.; Bonanno, A.; Xu, F. Study of band gap of silver nanoparticles—Titanium dioxide nanocomposites. J. Chem. 2014, (2014). https://doi.org/10.1155/2014/589707

[38]. Mie, G. Articles on the optical characteristics of turbid tubes, especially colloidal metal solutions. Ann. Phys. (1908). https://doi.org/10.1002/andp.19083300302

Devan Elumalaia, , Maduraiveeran Hemavathic, Chandrasekar Vijayalakshmi Deepaad, Patheri Kunyil Kaleenaa "Evaluation of phytosynthesised silver nanoparticles from leaf extracts of Leucas aspera and Hyptis suaveolens and their larvicidal activity against malaria, dengue and filariasis vectors", Parasite Epidemiology and Control 2 (2017) . doi: 10.1016/j.parepi.2017.09.001

Maryam Abdollahnia1, Ali Makhdoumi,Mansour Mashreghi1,2, Hossein Eshghi"Exploring the potentials of halophilic prokaryotes from a solar saltern for synthesizing nanoparticles: The case of silver and selenium", PLOS ONE https://doi.org/10.1371/journal.pone.0229886 March 4, (2020).

R. Palani velana, P.M. Ayyasamya , R. Kathiravanb , B. Subashni "Rapid decolorization of synthetic melanoidin by bacterial extract and their mediated silver nanoparticles as support" , Journal of Applied Biology & Biotechnology Vol. 3 (02), pp. 006-011, (2015). DOI: 10.7324/JABB.2015.3202

Z. Paranga , A. Keshavarzb,∗, S. Farahi c, S.M. Elahi a, M. Ghorannevissa, S. Parhoodehd"Fluorescence emission spectra of silver and silver/cobalt nanoparticles" Scientia Iranica, Transactions F: Nanotechnology 19 (2012) . doi:10.1016/j.scient.2012.02.026

C. Van der Horst, B. Silwana, E. Iwuoha & V. Somerset "Synthesis and Characterization of Bismuth- Silver Nanoparticles for Electrochemical Sensor Applications" Analytical Lett. https://doi.org/10.1080/00032719.2014.979357 (2015).

Enza Fazio , Bilal Gökce, Alessandro De Giacomo, Moreno Meneghetti, Giuseppe Compagnini, Matteo Tommasini, Friedrich Waag, Andrea Lucotti, Chiara Giuseppina Zanchi, Paolo Maria Ossi, Marcella Dell'Aglio, Luisa D'Urso, Marcello Condorelli , Vittorio Scardaci , Francesca Biscaglia, Lucio Litti, Marina Gobbo, Giovanni Gallo, Marco Santoro, Sebastiano Trusso and Fortunato Neri " Nanoparticles Engineering by Pulsed Laser Ablation in Liquids: Concepts and Applications" Nanomaterials 2020, 10, 2317; doi:10.3390/nano10112317

Kevin Kelly W. Edward Billups " Synthesis of Soluble Graphite and Graphene " November 2012. DOI: 10.1021/ar300121q